Multiparametric Phenotypic Screening System for Profiling Bioactive Compounds Using Human Fetal Hippocampal Neural Stem/Progenitor Cells

Yoshikuni Tabata[1], Norio Murai[1], Takeo Sasaki[2], Sachie Taniguchi[1], Shuichi Suzuki[1], Kazuto Yamazaki[1], and Masashi Ito[1]

Abstract

Stem cell research has been progressing rapidly, contributing to regenerative biology and regenerative medicine. In this field, small-molecule compounds affecting stem cell proliferation/differentiation have been explored to understand stem cell biology and support regenerative medicine. In this study, we established a multiparametric screening system to detect bioactive compounds affecting the cell fate of human neural stem/progenitor cells (NSCs/NPCs), using human fetal hippocampal NSCs/NPCs, HIP-009 cells. We examined effects of 410 compounds, which were collected based on mechanisms of action (MOAs) and chemotypes, on HIP-009's cell fate (self-renewal, neuronal and astrocytic differentiation) and morphology by automated multiparametric assays and profiled induced cellular phenotypes. We found that this screening classified compounds with the same MOAs into subgroups according to additional pharmacological effects (e.g., mammalian target of rapamycin complex 1 [mTORC1] inhibitors and mTORC1/mTORC2 dual inhibitors among mTOR inhibitors). Moreover, it identified compounds that have off-target effects under matrix analyses of MOAs and structure similarities (e.g., neurotropic effects of amitriptyline among tri- and tetracyclic compounds). Therefore, this automated, medium-throughput and multiparametric screening system is useful for finding compounds that affect the cell fate of human NSCs/NPCs for supporting regenerative medicine and to fingerprint compounds based on human stem cells' multipotency, leading to understanding of stem cell biology.

Introduction

Cytological phenotypic profiling based on a multiparametric high-content assay system is a powerful tool for characterization of compounds.[1,2] The phenotypes can be employed to classify bioactive compounds based on their mechanisms of action (MOAs) and also to detect or predict novel targets of compounds of which MOAs have not been clarified. By using human stem cells, we can make a novel physiologically relevant screening system that characterizes human cell-fate modulating profiles of compounds, because stem cells are pluripotent/multipotent, being different from using conventional cell lines. In the profiling assays with stem cells, detection of plural cell types by using phenotypic multicolor imaging with differentiation markers fits for this purpose. The results of the cell-fate analysis combined with high-content assays will be useful to understand basic stem cell biology and help regenerative medicine.[3,4]

In the brain, neural stem/progenitor cells (NSCs/NPCs) are unique, lifelong sources of both neurons and glia. Human NSCs/NPCs hold a great promise as a model for studying human neural biology and diseases, as a source of

[1]Next Generation Systems CFU, Eisai Product Creation Systems, Eisai Co., Ltd., Tokodai, Tsukuba, Ibaraki, Japan
[2]Global Discovery Research, Neuroscience and General Medicine PCU, Eisai Product Creation Systems, Eisai Co., Ltd., Tokodai, Tsukuba, Ibaraki, Japan

Corresponding Author:
Kazuto Yamazaki, Eisai Product Creation Systems, Eisai Co., Ltd., 5-1-3, Tokodai, Tsukuba, Ibaraki 300-2635, Japan.
Email: k5-yamazaki@hhc.eisai.co.jp

differentiated neural cells for regenerative medicine, and for bioassays for therapeutic efficacy and neuronal toxicity assessment during drug development. There are several types of NSCs/NPCs, such as fetal NSCs, adult NSCs, NSCs derived from embryonic stem cells (ESCs), induced pluripotent stem cells (iPSCs), and mesenchymal stem cells. We previously reported useful characteristics of HIP-009 cells, which are human fetal hippocampal NSCs/NPCs.[5] The cells can differentiate into functional neurons and astrocytes: they express functional glutamate receptors, such as *N*-methyl-D-aspartate (NMDA) receptors, α-amino-3-hydroxy-5-methyl-4-isoxazolepropionate receptors, and kainate receptors; neurons function electrophysiologically.

HIP-009 cells have the following unique features superior to the other human NSCs/NPCs. First, differentiated HIP-009 cells are considered to be a more physiologically relevant model as hippocampal neural cells (in other words, more region specific) than those derived from human ESCs/iPSCs, because HIP-009 cells themselves are originated from human hippocampal NSCs/NPCs. Second, HIP-009 cells can differentiate into both neurons and astrocytes simultaneously at an about equal ratio in the same culture system, while it is difficult for the other NSCs/NPCs. In this study, using these HIP-009 cells' features as NSCs/NPCs at maximum, we developed a multiparametric phenotypic assay system to screen compounds affecting cell fate (self-renewal of bipotent cells and differentiation into neurons and astrocytes) and morphology (e.g., neurite length and branch number) of HIP-009 cells. The results indicate that the multiparametric screening system can detect compounds having specific cell-fate modulating effects (e.g., neurotropic) and provide a novel fingerprinting method of compounds based on induced cellular phenotypes.

Materials and Methods

Chemicals

We constructed a bioactive compound library consisting of compounds whose MOAs have been known, collecting different chemotypes of compounds on the same MOA series to enable us to identify off-target effects. They were obtained by purchasing from Axon Medchem (Groningen, the Netherlands), Sigma-Aldrich (St. Louis, MO), Selleck Chemicals (Houston, TX), Wako (Osaka, Japan), and Shanghai Haoyuan Chemexpress (Shanghai, China). In addition, some compounds were synthesized in our laboratories (Tsukuba, Japan). We assayed 410 compounds of this library, which were numbered as 1 to 410. The mechanisms of compounds included enzyme (e.g., kinases) inhibitors and activators, agonists, antagonists, and modulators of receptors or channels. All compounds were dissolved in dimethyl sulfoxide (DMSO; Wako).

HIP-009 Cell Culture for Expansion

HIP-009 cells were purchased from GigaCyte (Branford, CT; now PhoenixSongs Biologicals, Branford, CT). Cells were expanded as described in the manufacturer's instructions. Dishes of 100 mm were coated with 10 µg/mL laminin (Sigma-Aldrich) in DMEM/Ham's F-12 (1:1; DMEM/F12; Wako). Cells were seeded and grown on these dishes in Neural StemCell Growth Medium (PhoenixSongs Biologicals) added with Neural StemCell Growth Supplement, 10 ng/mL basic fibroblast growth factor (bFGF), 20 ng/mL epidermal growth factor (EGF), 3 µM CHIR-99021, 1 µg/mL laminin, and 30 µg/mL gentamicin (Life Technologies, Carlsbad, CA). The medium was changed every 2 or 3 d, and confluent cells were split for expansion every 4 or 5 d. Cell culture was carried out at 37 °C in a humidified atmosphere of 2% O_2, balanced with N_2, and 6% CO_2. HIP-009 cells at passages 10 were used in assays. This study was performed with the approval of the Eisai Research Ethics Committee.

Validation of Cell-Fate Changes of HIP-009 Cells by Using Isoxazole-9

Creating the cell-fate modulator screening system using HIP-009 cells, we examined if we were able to detect phenotypic cell-fate changes of the cells by a reference compound in the assays. We used isoxazole-9 (*N*-cyclopropyl-5-[thiophen-2-yl]-isoxazole-3-carboxamide, Isx-9; Tocris Bioscience, Bristol, United Kingdom), which was reported to induce neuronal differentiation in rat hippocampal NSCs/NPCs.[6] Cell culture, immunostaining, imaging, and analysis procedures were basically the same as in the cell-fate screening described below.

Preparation of HIP-009 Cells for High-Content Screening

Expanded HIP-009 cells were harvested and suspended in Neural Transition Medium (PhoenixSongs Biologicals) added with Neural Transition Supplement, 10 ng/mL bFGF, 20 ng/mL EGF, 1 µg/mL laminin, and 30 µg/mL gentamicin and seeded on poly-D-lysine–precoated 96-well plates at $6 \times 10^3/100$ µL/well. One day after, the medium was exchanged into assay medium (DMEM/F12 supplemented with 1× N2 supplement [Wako], 1 µg/mL laminin, and 30 µg/mL gentamicin), and compounds were added at four concentrations of 10-fold serial dilution in reference to their cell toxicity ($n = 2$). DMSO-treated cells were used as a control ($n = 6$). The final concentration of DMSO was adjusted to 0.1% in all samples. Cells were treated with compounds for 7 d, and an additional 7 d culture was performed without compounds in the assay medium. Medium replacement was conducted every 3 or 4 d.

Immunostaining

After the 14 d assay treatment of cells, they were fixed with 1% paraformaldehyde (Wako) for 30 min at room temperature. After fixation, they were washed with phosphate-buffered saline (PBS; Wako) and permeabilized with 0.2% Triton X-100 (MP Biomedicals, Santa Ana, CA)/1× Blocking One (Nacalai tesque, Kyoto, Japan)/PBS (PBS-B-T buffer) for 30 min at room temperature. Then, cells were incubated with primary antibodies (goat anti-SOX1 [as a neural progenitor marker, 1:1000; R&D Systems, Minneapolis, MN], rat anti-GFAP [as an astrocyte marker, 1:1000; Life Technologies], and mouse anti-MAP2 [as a neuron marker, 1:1000; Sigma-Aldrich]) in PBS-B-T buffer overnight at 4 °C. After washing with 0.1% Tween-20 (Wako)/PBS, cells were treated with secondary antibodies (anti-goat IgG [H+L] Alexa Fluor 488 [1:500; Life Technologies], anti-rat IgG [H+L] Alexa Fluor 594 [1:500; Life Technologies], and anti-mouse IgG [H+L] Alexa Fluor 647 [1:500; Life Technologies]) and Hoechst-33342 (5 µg/mL; Sigma-Aldrich) in PBS-B-T buffer for 60 min at room temperature.

Imaging Analysis

Image acquisition and analysis were performed by CellVoyager6000 (CV6000), an automated high-throughput cytological discovery system with laser-scanning confocal microscopes and image analysis (Yokogawa Electric Corp., Tokyo, Japan). Four channels of excitation laser wavelength (405, 488, 561, and 635 nm) were used. A total of 45 fields per well were scanned at 10× magnification to produce a tiled image for whole-well image acquisition. The CV6000 quantified numbers of cells positive for SOX1, MAP2, and GFAP among total cells (Hoechst-33342). We calculated ratios of SOX1$^+$, MAP2$^+$, and GFAP$^+$ cell numbers to total cell numbers and used them in analyses. In addition, neurite arborization (neurite length and branching number) of MAP2$^+$ cells was quantified using an algorithm of the CV6000 software. The algorithm segmented the cells into nucleus-adjacent neuronal somas and neurite traces, further determining neurite branching points. This analysis was also applied to GFAP$^+$ cells. Then, the following morphological changes were calculated: neurite length per MAP2$^+$ cell, and process length per GFAP$^+$ cell; number of neurite branching per MAP2$^+$ cell, and number of process branching per GFAP$^+$ cell. Image analysis extracting the cell population and morphology is shown in **Supplemental Figure S1**.

Data Analysis

In the preliminary study to validate effects of Isx-9 on phenotypic changes of HIP-009 cells in the assay procedures, one-way analysis of variance was performed, followed by Dunnett's multiple comparison test as a post hoc test, comparing with the DMSO-treated group. Probability (p) values <0.05 were considered statistically significant.

Collected data of the screening were expressed as fold changes relative to those of the DMSO-treated control group. Criteria for selecting significant changes were set as ≥3× Z-score or ≤–3× Z-score. Data at concentrations showing <50% cell viability were excluded. When the same direction of parameter changes (increases [≥3× Z-score] or decreases [≤–3× Z-score]) was observed at two or more concentrations of a compound, this change was regarded as a specific phenotype of this compound. The changes were ranked as ≥3, ≥5 and ≥10 for increases and ≤–3, ≤–5 and ≤–10 for decreases. The maximum or minimum change of a compound was used in fingerprinting and phenotypic clustering. Dendrograms of compounds' phenotypes were produced based on clustering and distance measurement by using the complete linkage and cosine correlation, respectively. A hierarchical chemical structure clustering was made based on the Tanimoto similarity between the chemical fingerprinting. The phenotypic and chemical clustering and dendrogram drawing were performed by using TIBCO Spotfire software (TIBCO Software Inc., Palo Alto, CA).

Results

Phenotypic Changes of HIP-009 Cells by Isx-9

Total cell numbers were significantly decreased by Isx-9 at 3.3 ($p < 0.05$) and 10 µM ($p < 0.001$; **Fig. 1A**). SOX1$^+$ cell number was significantly increased at 3.3 µM ($p < 0.05$; **Fig. 1B**). A trend in an increase of SOX1$^+$ cells was observed at 1.1 µM ($p = 0.0932$) and 10 µM ($p = 0.0600$). GFAP$^+$ cell number was decreased concentration dependently (**Fig. 1C**). There was no significant change of GFAP$^+$ cell process length, but a significant reduction of GFAP$^+$ cell process branch number was seen at 10 µM ($p < 0.01$; data not shown). Isx-9 increased MAP2$^+$ cell number (**Fig. 1D**), and MAP2$^+$ neurite length (**Fig. 1E**) and branch number (**Fig. 1F**) in a concentration-dependent manner. Moreover, a trend in increases of MAP2$^+$ cell neurite length and branch number was seen at 1.1 µM ($p = 0.0531$ for neurite length; $p = 0.0507$ for neurite branch number).

Cell-Fate Screening: General Observations

We counted the total cell number as one phenotypic parameter in this screening. Twenty compounds showing <50% cell viability at three or four concentrations were excluded in further analysis. Of the remaining 390 compounds, 148 compounds manifested no phenotypic change. **Figure 2A** indicates a dendrogram of 242 compounds drawn based on the phenotypes of HIP-009 cells. The graph demonstrated
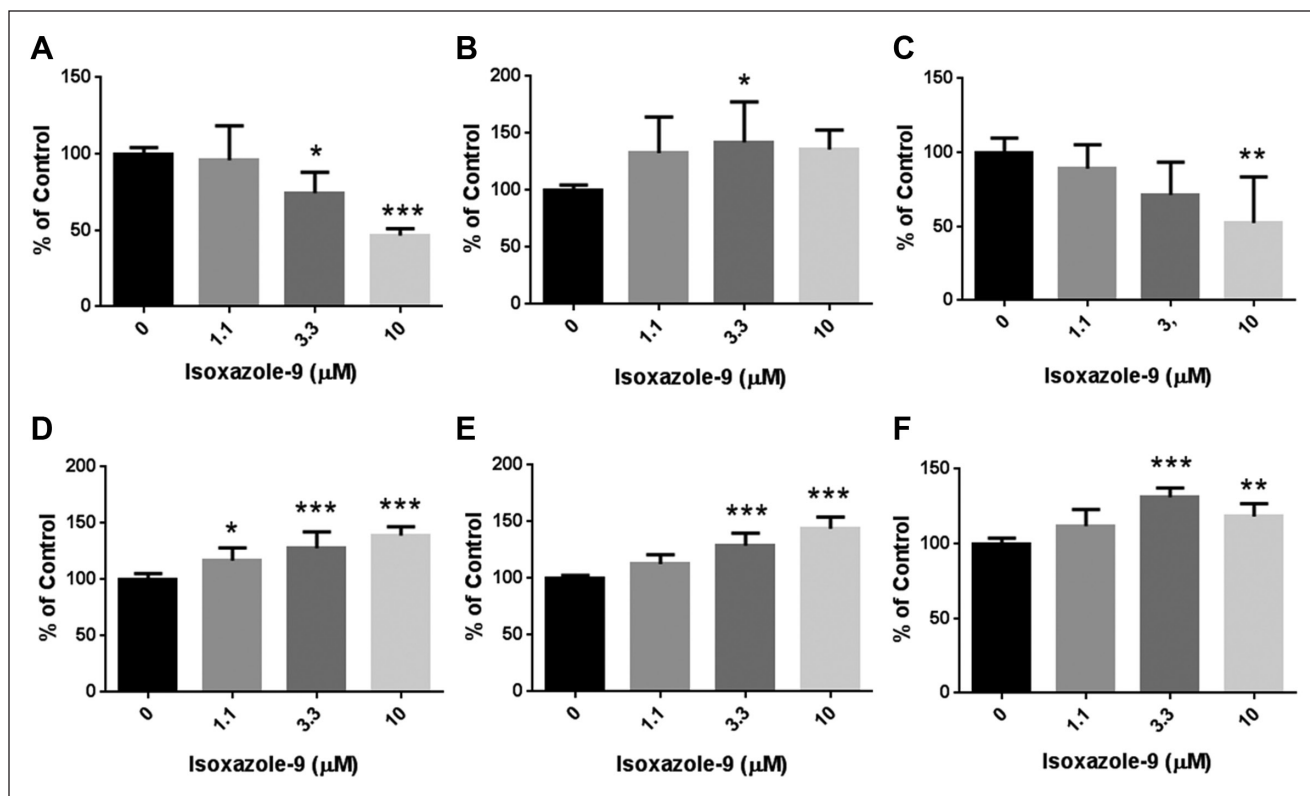
Figure 1. Validation of neurotropic effects of isoxazole-9 (*N*-cyclopropyl-5-[thiophen-2-yl]-isoxazole-3-carboxamide) on human neural stem/progenitor cells, HIP-009 cells, for the construction of cell-fate screening system. HIP-009 cells were treated with isoxazole-9 (1.1 μM, 3.3 μM, or 10 μM) or vehicle (dimethyl sulfoxide) according to the Materials and Methods section. We quantified total, SOX1^{+}, MAP2^{+}, and GFAP[+] cell numbers; MAP2^{+} cell neurite length and branch number; and GFAP[+] process length and branch number. Regarding SOX1^{+}, MAP2^{+}, and GFAP[+] cell number, we compared ratios of numbers of cells positive for these markers to total cell numbers. (**A**) Total cell number. (**B**) SOX1^{+} cell number. (**C**) GFAP[+] cell number. (**D**) MAP2^{+} cell number. (**E**) Neurite length of MAP2^{+} cells. (**F**) Neurite branch number of MAP2^{+} cells. Data are means ± standard deviation. Isoxazole-9 (0 μM; vehicle), *n* = 7; isoxazole-9 (1.1 μM), *n* = 4; isoxazole-9 (3.3 μM), *n* = 4; isoxazole-9 (10 μM), *n* = 4. Values are evaluated by one-way analysis of variance, followed by Dunnett's multiple comparison test. *$p < 0.05$; **$p < 0.01$; ***$p < 0.001$.

that we were able to group compounds into several clusters according to the phenotypes. We analyzed correlations between two phenotypic parameters by drawing scatter plots (**Suppl. Fig. S2**). Generally speaking, the correlations did not seem to be so high, but there was an exceptional case, that is, between MAP2^{+} cell neurite length and branch number. By drawing regression lines, we calculated correlation coefficients between the parameters, and the highest correlation coefficient was observed between MAP2^{+} cell neurite length and branch number (**Suppl. Fig. S3**). **Figure 2B** shows representative compounds affecting numbers of MAP2^{+} and GFAP^{+} cells. GSK3 inhibitors (#9 [CHIR-99021] and #100 [AZD2858]), a BMP receptor (ALK2/3) inhibitor (#62 [LDN-193189]), and a STAT3 inhibitor (#152 [WP1066]) increased MAP2^{+} cell number. LDN-193189, WP1066, and #154 (S3I-201, a STAT3 inhibitor) decreased GFAP[+] cell number. On the other hand, mammalian target of rapamycin complex 1 (mTORC1) inhibitors (#146 (sirolimus [rapamycin]), #28

[temsirolimus], and #39 [everolimus]), MEK inhibitors (#25 [PD0325901] and #61 [TAK-733]), and p38 MAPK inhibitors (#72 [PH-797804], and #387 [SB203580]) lowered MAP2^{+} cell number. The two MEK inhibitors increased GFAP[+] cell number.

Cell-Fate Screening: Specified Observation Examples

Applying the phenotypic clustering to specific subjects, such as compound groups with similar MOAs and chemical structures, we found several interesting observations, demonstrating further value as a unique screening system. We describe results of some examples hereafter. Compounds selected for specified observations are listed in **Supplemental Table S1**, along with their concentrations used for phenotypic fingerprinting.
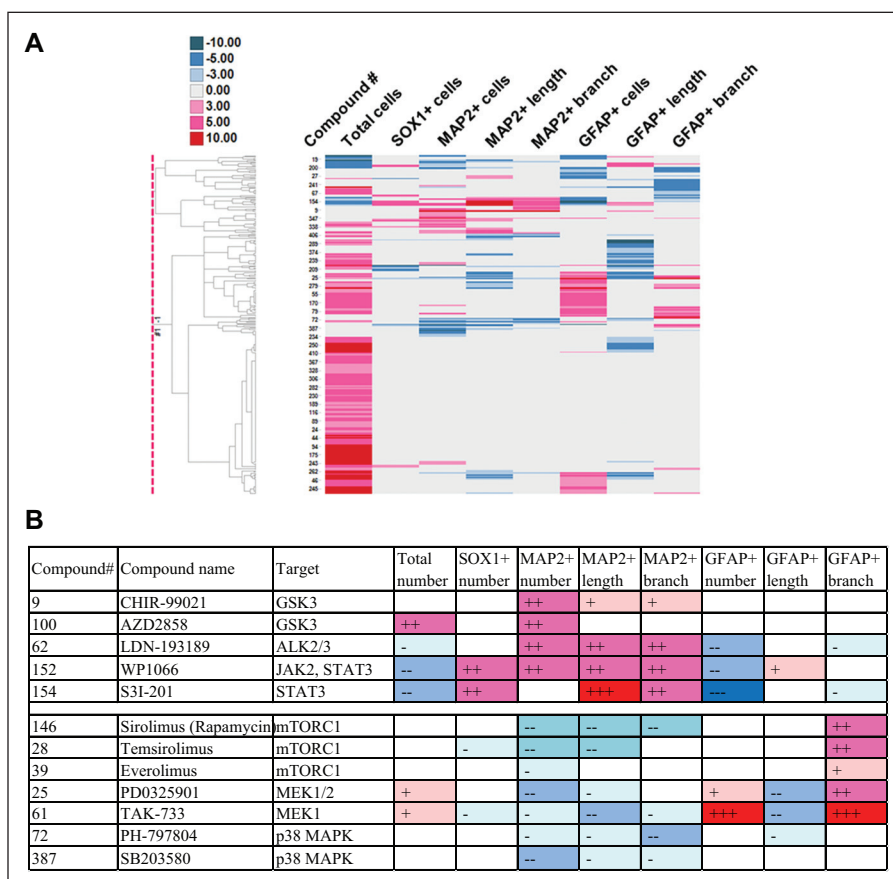
Figure 2. (**A**) Dendrograms and phenotypic clustering of 242 compounds according to HIP-009 cells' phenotypes. Changes of phenotypic parameters ≥3× Z-score or ≤−3× Z-score are considered significant. The changes are graded as follows: 0 (not significant); ≥3, ≥5×, and ≥10× Z-score for increases; ≤−3×, ≤−5×, and ≤−10× Z-score for decreases. All compound numbers are not described. (**B**) Fingerprints of representative compounds increasing or decreasing MAP2^{+} or GFAP[+] cell number of HIP-009 cells. +, ++, +++, −, − −, and − − − indicate ≥3×, ≥5×, ≥10×, ≤−3×, ≤−5×, and ≤−10× Z-score, respectively. Color is also added in this table: red and blue become darker as the changes are larger.

Compound#	Compound name	Target	Total number	SOX1+ number	MAP2+ number	MAP2+ length	MAP2+ branch	GFAP+ number	GFAP+ length	GFAP+ branch
9	CHIR-99021	GSK3			++	+	+			
100	AZD2858	GSK3	++		++					
62	LDN-193189	ALK2/3	-		++	++	++	--		-
152	WP1066	JAK2, STAT3	--	++	++	++	++	--	+	
154	S3I-201	STAT3	--	++		+++	++	---		-
146	Sirolimus (Rapamycin)	mTORC1			--	--	--			++
28	Temsirolimus	mTORC1		-	--	--				++
39	Everolimus	mTORC1			-					+
25	PD0325901	MEK1/2	+		--	-		+	--	++
61	TAK-733	MEK1	+	-	-	-	-	+++	--	+++
72	PH-797804	p38 MAPK			-	-	-		-	
387	SB203580	p38 MAPK			--	-	-			

Profiling of Tri- and Tetracyclic Compounds Used for Mental Disorders

Supplemental Figure S4 shows the chemical structures of tri- and tetracyclic compounds, which are prescribed as drugs for mental disorders. Phenotypic clustering of these compounds is indicated in **Figure 3A**. Interestingly, only #347 (amitriptyline hydrochloride [AMT]) displayed a unique neurotropic fingerprint: a prominent increase of MAP2^{+} cell number and increases of MAP2^{+} cell neurite length and branch number, shown in the bottom row of **Figure 3A**. Structure clustering demonstrated that AMT, #367 (nortriptyline hydrochloride), #368 (doxepin hydrochloride), and #372 (maprotiline hydrochloride) made one cluster (**Fig. 3B**). However, the phenotypes of nortriptyline, doxepin, and maprotiline differed from those of AMT (an increase of total cell number for nortriptyline, increases of total and SOX1^{+} cell numbers for doxepin, and no phenotypic change for maprotiline; **Fig. 3A**).

There are several MOAs of tricyclic and tetracyclic antidepressants, including inhibition of serotonin transporter and of norepinephrine transporter, antagonism at 5-HT$_2$ (5-HT$_{2A}$ and 5-HT$_{2C}$), 5-HT$_6$, 5-HT$_7$, α_1-adrenergic and NMDA receptors, and agonism at σ receptors. AMT works as a serotonin-norepinephrine reuptake inhibitor (SNRI),[7] and also as an antagonist at 5-HT$_{2A}$ and 5-HT$_{2C}$ receptors.[8] **Supplemental Table S2** shows phenotypic profiles of selective serotonin reuptake inhibitors (SSRIs), SNRIs, norepinephrine reuptake inhibitors (NRIs), and antagonists at 5-HT$_{2A}$ and 5-HT$_{2C}$ receptors of other compounds than tri- and tetracyclic compounds. There was no compound manifesting the same profiles as AMT.

Profiling of mTOR Inhibitors

Chemical structures of mTOR inhibitors are pictured in **Supplemental Figure S5**, and their phenotypic fingerprinting is illustrated in **Figure 4A**. **Figure 4B** shows phenotypic clustering of the mTOR inhibitors. We observed two main groups in the clustering: one group showed common phenotypes of increases of total and GFAP[+] cell numbers and the other displayed a decrease of MAP2^{+} cell number. Intriguingly, the former group included mTORC1/mTORC2 dual inhibitors (#185 [WYE-12532], #145 [PP242], #140 [Ku-0063794], and #174 [AZD8055]) and an mTOR/PI3K dual inhibitor (#75 [PF-04691502]). This phenotypically similar group was divided into two structural clusters: one included PP242 and WYE-12532, and the other did
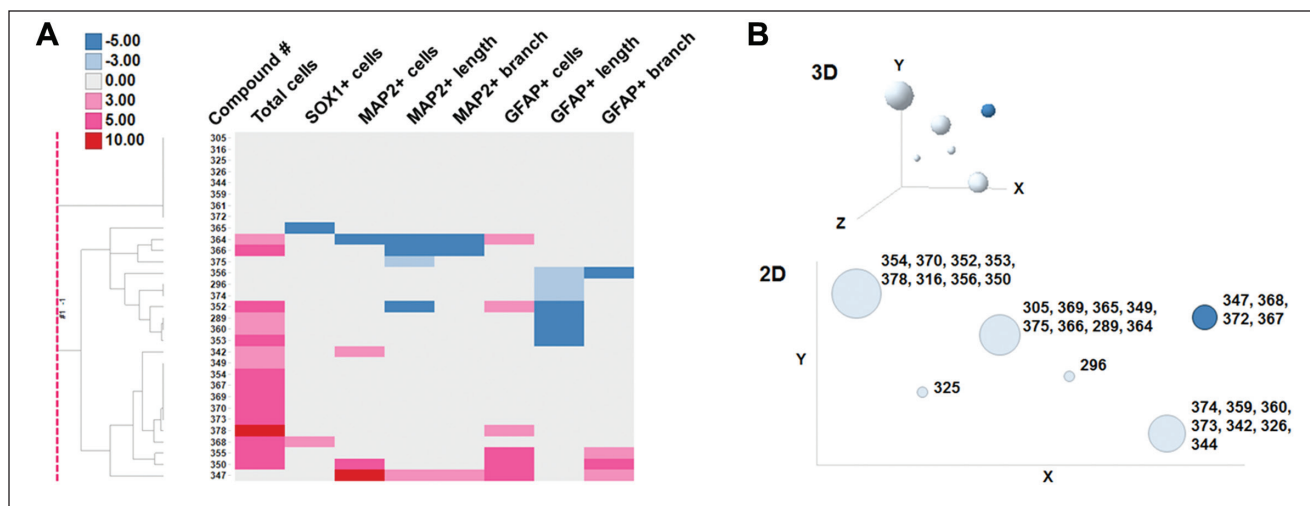
Figure 3. (**A**) Dendrograms of phenotypic clustering of tri- and tetracyclic compounds based on HIP-009 cells' phenotypes. Changes of phenotypic parameters ≥3× Z-score or ≤−3× Z-score are considered significant. The changes are graded as follows: 0 (not significant); ≥3×, ≥5×, and ≥10× Z-score for increases; ≤−3×, ≤−5×, and ≤−10× Z-score for decreases. Note that only #347 (amitriptyline hydrochloride) shows a unique neurotropic phenotype: increases of MAP2$^+$ cell number and MAP2$^+$ cell neurite length and branch number in the bottom row. (**B**) Three-dimensional and two-dimensional structure clustering of the tri- and tetracyclic compounds. Blue sphere and circle indicate one cluster containing amitriptyline. Numbers by circles show compounds' numbers included in the circles (clusters).

PF-04691502, Ku-0063794, and AZD8055 (**Fig. 4C**). The latter group of phenotypic clustering included mTORC1 inhibitors (#146 [sirolimus {rapamycin}], #28 [temsirolimus], and #39 [everolimus]). Temsirolimus and everolimus are rapamycin analogs, that is, rapalogs. Interestingly, #151 (compound 401) manifested unique phenotypes among the mTOR inhibitors examined: an increase of SOX1$^+$ cell number and a decrease of GFAP$^+$ cell branch number, although this compound was included in a structurally similar cluster containing pyrazolopyrimidine derivatives (PP242 and WYE-125132) and triazolopyrimidine derivative (#74 [PKI-402]).

Profiling of Dopamine Receptor Agonists

Among the bioactive compounds assayed in this screening, there were seven dopamine receptor agonists. These compounds were classified into two groups based on their structures: ergoline derivatives (#264 [pergolide mesylate], #278 [bromocriptine mesylate], #279 [lisuride maleate], and #298 [metergoline]), and nonergoline derivatives (#282 [ropinirole hydrochloride], #290 [talipexole dihydrochloride], and #291 [pramipexole hydrochloride]]). The chemical structures of these compounds are in **Supplemental Figure S6**. Their structure clustering is shown in **Figure 5A**. Phenotypically, there were two groups: one showed increases of total and GFAP$^+$ cell numbers and a decrease of MAP2$^+$ neurite length; the other showed an increase of total cell number only (**Fig. 5B**). The former and latter phenotypic clusters consisted of ergoline (pergolide, bromocriptine, and

lisuride) and nonergoline derivatives (ropinirole, talipexole, and pramipexole), respectively. Metergoline did not display any change of the parameter, although it is an ergoline derivative.

Discussion

In constructing the cell-fate multiparametric phenotypic screening, we used Isx-9 as a reference compound to examine if the assay was able to detect HIP-009 cells' phenotypic changes by this compound as previously reported. Isx-9 was identified as a small-molecule compound to trigger neuronal differentiation in adult rat hippocampal NSCs/NPCs.[6] Moreover, mice treated with Isx-9 showed proliferation and neurogenesis in the hippocampal subgranular zone (SGZ), accompanied with enhanced dendrite arborization including dendrite length and branching.[9] In our study, Isx-9 induced concentration-dependent increases of the MAP2$^+$ cell population and MAP2$^+$ cell neurite length and branch number in HIP-009 cells. Thus, these phenotypes were matched with the in vitro and in vivo changes caused by Isx-9 in rodents, suggesting that Isx-9 is also neurotropic in humans. Furthermore, it was reported that Isx-9 inhibited astrocyte differentiation induced by leukemia inhibitory factor and BMP-2.[7] It appeared that GFAP$^+$ cells were decreased in a concentration-dependent manner in our examination. These results of the validation experiment using Isx-9 would promise us to detect cell-fate and morphological changes of human NSCs/NPCs by bioactive compounds in the procedures of the screening.
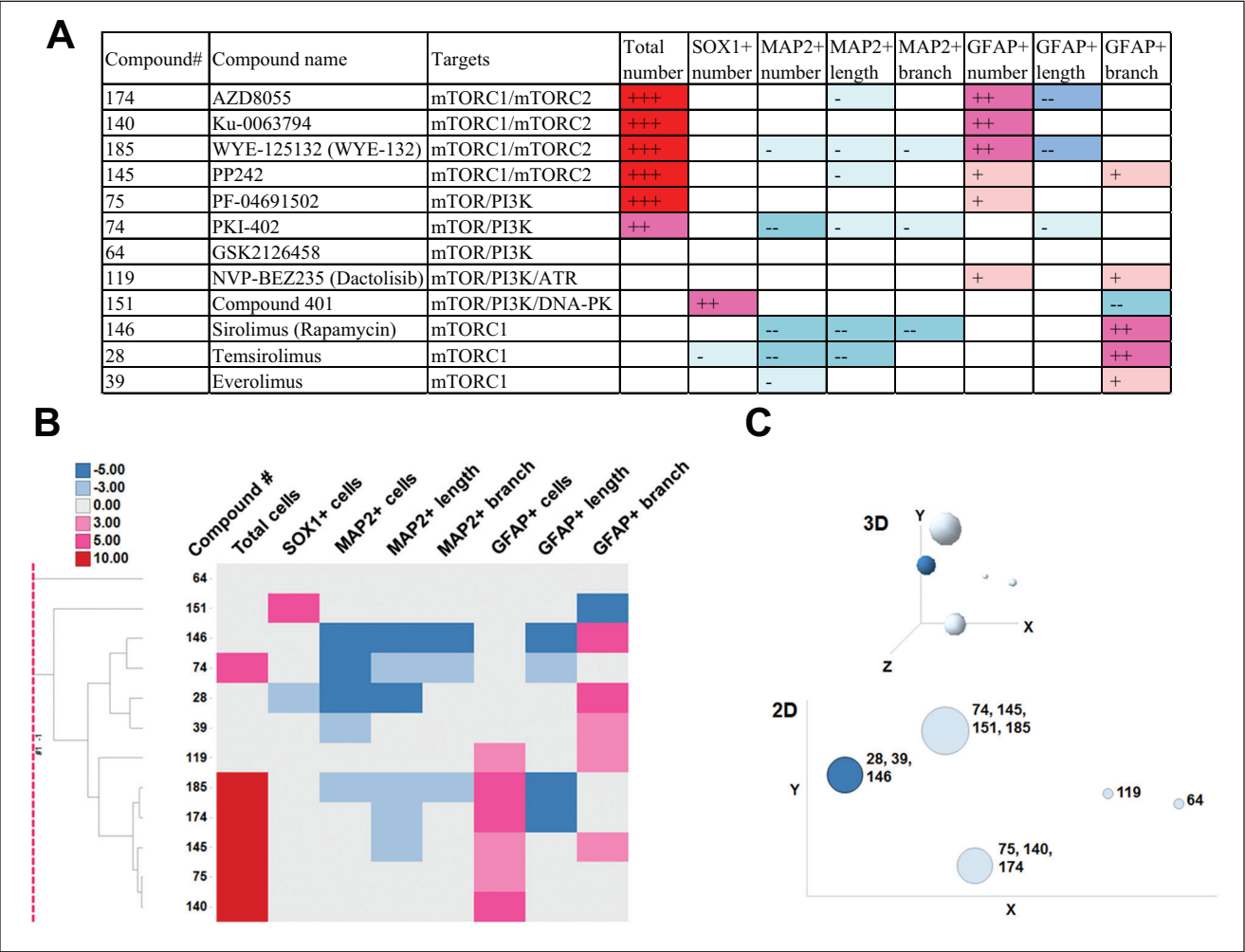
A

Compound#	Compound name	Targets	Total number	SOX1+ number	MAP2+ number	MAP2+ length	MAP2+ branch	GFAP+ number	GFAP+ length	GFAP+ branch
174	AZD8055	mTORC1/mTORC2	+++			-		++	--	
140	Ku-0063794	mTORC1/mTORC2	+++					++		
185	WYE-125132 (WYE-132)	mTORC1/mTORC2	+++		-	-	-	++	--	
145	PP242	mTORC1/mTORC2	+++					+		+
75	PF-04691502	mTOR/PI3K	+++					+		
74	PKI-402	mTOR/PI3K	++		--	-	-		-	
64	GSK2126458	mTOR/PI3K								
119	NVP-BEZ235 (Dactolisib)	mTOR/PI3K/ATR						+		+
151	Compound 401	mTOR/PI3K/DNA-PK		++						--
146	Sirolimus (Rapamycin)	mTORC1			--	--	--			++
28	Temsirolimus	mTORC1		-	--	--				++
39	Everolimus	mTORC1			-					+

B

C

Figure 4. (**A**) Fingerprinting of mTOR inhibitors based on HIP-009 cells' phenotypes. Changes of phenotypic parameters $\geq 3\times$ Z-score or $\leq -3\times$ Z-score are considered significant. The changes are graded as followed: 0 (not significant); $\geq 3\times$, $\geq 5\times$, and $\geq 10\times$ Z-score for increases; $\leq -3\times$, $\leq -5\times$, and $\leq -10\times$ Z-score for decreases. +, ++, +++, −, and − − indicate $\geq 3\times$, $\geq 5\times$, $\geq 10\times$, $\leq -3\times$, and $\leq -5\times$ Z-score, respectively. Color is also added in this table: red and blue become darker as the changes are larger. (**B**) Dendrograms and phenotypic clustering of the mTOR inhibitors according to their phenotypes. (**C**) Results of three-dimensional and two-dimensional structure clustering. Blue sphere and circle indicate one cluster including sirolimus (rapamycin) and two rapalogs (temsirolimus and everolimus). Numbers by circles indicate compound numbers included in the circles (clusters).

We showed representative compounds having an influence on MAP2⁺ or GFAP⁺ cell numbers (**Fig. 2B**). These results were in a good agreement of the following published findings: a dominant negative Stat3 mutant increased MAP2 protein levels and MAP2⁺ cell numbers but decreased GFAP protein levels and GFAP⁺ cell number in rat fetal NSCs[10]; cyclic adenosine monophosphate and nerve growth factor–induced neuronal differentiation and neurite outgrowth were inhibited by SB203580 at 1 and 10 μM in rat pheochromocytoma PC12 cells[11]; CHIR-99021 treatment at 3 μM promoted neuronal differentiation from human iPSC-derived NPCs,[12] and other GSK3 inhibitors, SB216763 (3 μM) and kenpaullone (1 μM), accelerated neurogenesis of a human immortalized NPC line, ReNcell VM[13]; rapamycin at 5 μM abrogated insulin-induced neuronal differentiation

in rat neonatal NPCs[14]; BMP-4 induced astrocyte differentiation of NSCs/NPCs collected from the subventricular zone (SVZ) of fetal mice[15] and rats[16]; exposure of BMP-2 to mouse fetal telencephalic NPCs caused developmental fate change from neurons to astrocytes[17]; microinjection of an MEK inhibitor, U0126, into the caudate-putamen and SGZ resulted in a decreases in NSCs and NeuN⁺ cells in the SGZ and SVZ of C57BL/6J mice aged 3 mo.[18] The scheme of the pathways with the inhibitors used in this screening is indicated in **Figure 6**. As in the references cited above, these pathways seem to be common between humans and rodents. In addition, these results validated the screening system as cell-fate assays using neural stem/progenitor cells.

Results of scatter plots and correlation coefficients of the phenotypic parameters indicated that the correlations
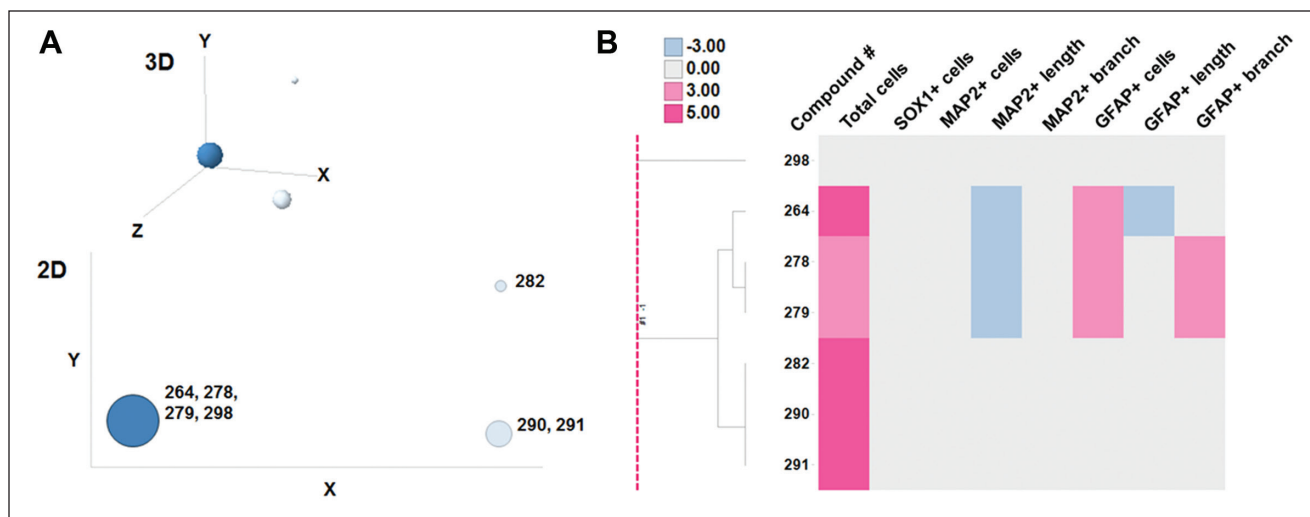
Figure 5. (**A**) Three-dimensional and two-dimensional structure clustering, showing that ergoline derivatives make one cluster (blue sphere and circle). Numbers by circles indicate compound numbers included in the circles (clusters). (**B**) Dendrograms and phenotypic clustering of the dopamine receptor agonists based on HIP-009 cells' phenotypes. Changes of phenotypic parameters ≥3× Z-score or ≤−3× Z-score are considered significant. The changes are graded as follows: 0 (not significant); ≥3×, ≥5×, and ≥10× Z-score for increases; ≤−3×, ≤−5×, and ≤−10× Z-score for decreases.

between two parameters were not so high each other, excluding a case between MAP2$^+$ cell neurite length and branch number (**Suppl. Figs. S2 and S3**). This means that the phenotypic parameters in this screening are not biased to particular cellular phenomena. Thus, it is suggested that using these parameters enables us to catch a wide range of cellular physiological reactions to compounds in one screening, having the advantage for phenotypic fingerprinting of compounds.

We found the unique phenotypic fingerprint of AMT among the tri- and tetracyclic compounds: a prominent increase of MAP2$^+$ cell number with increases of MAP2$^+$ neurite length and branch number (**Fig. 3A**). AMT is a tricyclic antidepressant, and its main MOA is serotonin-norepinephrine reuptake inhibition, also antagonizing activity against 5-HT$_{2A}$ and 5-HT$_{2C}$ receptors. Besides AMT, #349 (imipramine hydrochloride), #370 (dosulepin hydrochloride), and nortriptyline act as SNRIs, but their phenotypic profile was an increase of total cell number. Furthermore, we picked up phenotypic profiles of compounds used for mental disorders whose MOAs are related to serotonin and/ or norepinephrine (SSRIs, SNRIs, and NRIs) and to antagonism at 5-HT$_{2A}$ and 5-HT$_{2C}$ receptors. But there were no compounds showing phenotypes similar to AMT (**Suppl. Table S2**). Therefore, it is less likely that the AMT's unique profile is due to its major MOAs as antidepressants.

The neurotropic effects of AMT were reported both in vitro and in vivo. Potentiated neurite formation and axonal growth of primary mouse hippocampal or cortical neurons by AMT at 10 nM were reported by Chadwick et al.[19] In addition, they showed cognitive enhancement with neurogenesis in transgenic Alzheimer's disease model mice treated with AMT. Jang et al.[20] reported that AMT was a TrkA and TrkB receptor agonist, demonstrating significant neurite outgrowth in PC12 cells at 100 to 500 nM. They reported that neurite outgrowth was not induced by the following tricyclic antidepressants: imipramine, chlorimipramine, prochlorperazine, promazine, trimeprazine or quinacrine. Among them, imipramine, chlorimipramine (#369), promazine (#316), and prochlorperazine (#378) were characterized in our phenotypic screening, and no compounds increased MAP2$^+$ cell number, neurite length, or branch number (**Fig. 3A**). Thus, it is possible that AMT manifests remarkable neurotropic effects via TrkA and/or TrkB receptor in the screening. In other words, this screening system is able to detect neurotropic compounds definitely, although it is a pinpointed, off-target action.

We presented here phenotypic fingerprinting results of compounds having inhibitory activity against mTOR. Sato et al.[21] reported that inhibition of either PI3K by LY294002 (5 μM) or mTOR by rapamycin (10–50 nM) reduced mouse fetal NSCs/NPCs and did not affect self-renewal potency. However, when both PI3K and mTOR were inhibited at the same time, the cells moved into astrocytic differentiation, judged by GFAP expression. An mTOR/PI3K dual inhibitor, PF-04691502, increased GFAP$^+$ cell number in our screening (**Fig. 4A**), which is in agreement with the observation by Sato et al. Four mTORC1/mTORC2 dual inhibitors (AZD8055, Ku-0063794, WYE-125132, and PP242) displayed phenotypes common to those of PF-04691502 (increases of total and GFAP$^+$ cell numbers), which were not induced by mTORC1 inhibitors (sirolimus, temsirolimus, and everolimus). Chronic
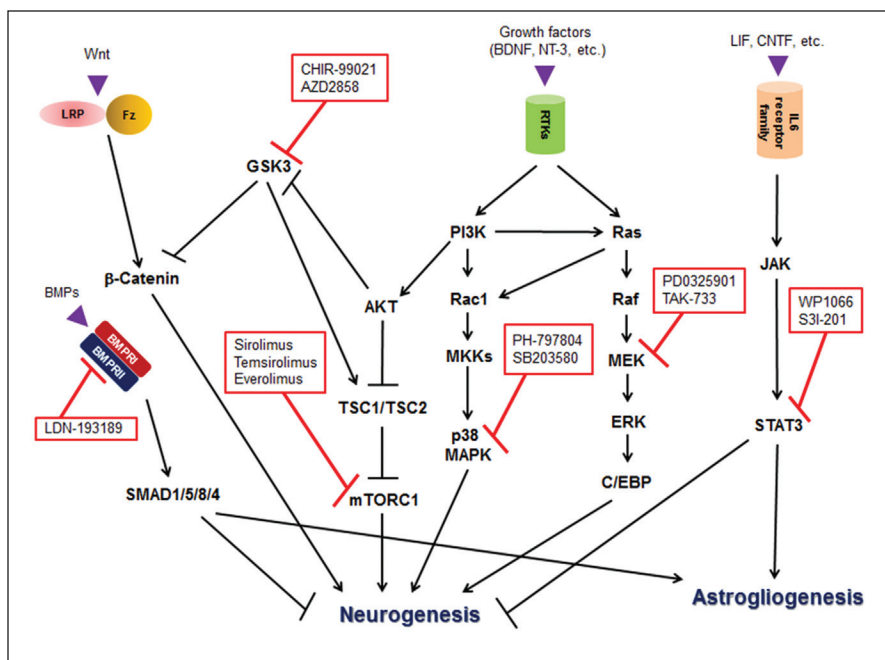
Figure 6. The diagram of the expected regulation of neurogenesis and astrogliogenesis based on the results of the compounds listed in **Figure 2B**. BDNF, brain-derived neurotrophic factor; BMP, bone morphogenetic protein; BMPR, BMP receptor; CNTF, ciliary neurotrophic factor; C/EBP, CCAAT-enhancer-binding protein; Fz, Frizzled; GSK3, glycogen synthase kinase 3; JAK, Janus kinase; LIF, leukemia inhibitory factor; LRP, lipoprotein receptor-related protein; MEK/MKK, mitogen-activated protein kinase kinase; mTORC1, mammalian target of rapamycin complex 1; NT-3, neurotrophin-3; RTK, receptor tyrosine kinase; SMAD1/5/8/4, SMAD family member 1/5/8/4; STAT3, signal transducer and activator of transcription 3; TSC1/2, tuberous sclerosis complex 1/2.

rapamycin treatment at 100 nM to mouse NSCs resulted in complete abrogation of neuronal differentiation.[22] All mTORC1 inhibitors reduced MAP2$^+$ cell number, which accords with this report. mTORC2 pathway regulation has not been fully elucidated, compared with mTORC1.[23] The present results suggest that target(s) of mTORC2 would be located upstream of mTORC1 in the PI3K pathway, such as AKT.

We can divide dopamine receptor agonists into two groups according to HIP-009 cells' phenotypic profiles. One group increased total cells and GFAP$^+$ cells, and decreased MAP2$^+$ cell neurite length, whereas the other group increased total cell number only (**Fig. 5B**). Of interest, all compounds in the former group were ergoline derivatives, and the latter's compounds were nonergoline derivatives. Pertz and Eich[24] described that bromocriptine and lisuride were partial agonists at dopamine D_2 receptors, and pergolide showed mixed agonistic activity of dopamine D_1 and D_2 receptors. On the other hand, Tadori et al.[25] showed that ropinirole, talipexole, pramipexole, bromocriptine, and pergolide behaved as dopamine D_2 and D_3 receptor full agonists. Metergoline is categorized not only as a dopamine receptor agonist[26,27] but also as a 5-HT$_{2C}$/5-HT$_{1B}$/5-HT$_{1D}$ ligand.[24] It was reported that bromocriptine had affinity for 5-HT$_{1A}$ receptors and lisuride had affinity for 5-HT$_{1A}$, 5-HT$_{1D}$, 5-HT$_{2A}$, 5-HT$_{2B}$, and 5-HT$_{2C}$ receptors. Pertz and Eich[24] then wrote that ergoline derivatives were "dirty" drugs. It is thus possible that phenotypic grouping results of these dopamine receptor agonists are due to these pharmacological characteristics derived from their structures.

Heilker et al.[28] described that there was no publication of a high-throughput screening campaign using expandable human NPCs, but they cited two pilot-scale screenings using human iPSC-derived NSCs/NPCs. As differentiation from NSCs/NPCs into neural cells is time-consuming, it is difficult to make cell-fate assays high throughput. We believe that how many valuable and unique parameters we can collect from one assay is very important. Thus, multiparametric screening is fit for this purpose. In the combination of multiparametric phenotyping and characteristics of HIP-009 cells as human expandable NSCs/NPCs, we developed the automated medium-throughput, multiparametric phenotypic screening in this study. This screening is a unique, powerful approach to detect compounds to modify the cell fate of human NSCs/NPCs for helping make progress in regenerative medicine and understand stem cell biology well. In addition, it is very useful as a phenotypic fingerprinting method to categorize compounds according to MOAs and to find compounds with novel, off-target effects among the compounds with the same MOA, using the compound library with a variety of chemotypes.

Declaration of Conflicting Interests

Funding

References

1. Young, D. W.; Bender, A.; Hoyt, J.; et al. Integrating High-Content Screening and Ligand-Target Prediction to Identify Mechanism of Action. *Nat. Chem. Biol.* **2008**, *4*, 59–68.

2. Woehrmann, M. H.; Bray, W. M.; Durbin, J. K.; et al. Large-Scale Cytological Profiling for Functional Analysis of Bioactive Compounds. *Mol. BioSyst*. **2013**, *9*, 2604–2617.

3. Li, W.; Jiang, K.; Ding, S. A Chemical Approach to Control Cell Fate and Function. *Stem Cells* **2012**, *30*, 61–68.

4. Längle, D.; Halver, J.; Rathmer, B.; et al. Small Molecules Targeting In Vivo Tissue Regeneration. *ACS Chem. Biol*. **2014**, *9*, 57–71.

5. Fukushima, K.; Tabata, Y.; Imaizumi, Y.; et al. Characterization of Human Hippocampal Neural Stem/Progenitor Cells and Their Application to Physiologically Relevant Assays for Multiple Ionotropic Glutamate Receptors. *J. Biomol. Screen*. **2014**, *19*, 1174–1184.

6. Schneider, J. W.; Gao, Z.; Li, S.; et al. Small-Molecule Activation of Neuronal Cell Fate. *Nat. Chem. Biol*. **2008**, *4*, 408–410.

7. Tatsumi, M.; Groshan, K.; Blakely, R. D.; et al. Pharmacological Profile of Antidepressants and Related Compounds at Human Monoamine Transporters. *Eur. J. Pharmacol*. **1997**, *340*, 249–258.

8. Werling, L. L.; Keller, A.; Frank, J. G.; et al. A Comparison of the Binding Profiles of Dextromethorphan, Memantine, Fluoxetine and Amitriptyline: Treatment of Involuntary Emotional Expression Disorder. *Exp. Neurol*. **2007**, *207*, 248–257.

9. Petrik, D.; Jiang, Y.; Birnbaum, S. G.; et al. Functional and Mechanistic Exploration of an Adult Neurogenesis-Promoting Small Molecule. *FASEB J*. **2012**, *26*, 3148–3162.

10. Gu, F.; Hata, R.; Ma, Y.J.; et al. Suppression of Stat3 Promotes Neurogenesis in Cultured Neural Stem Cells. *J. Neurosci. Res*. **2005**, *81*, 163–171.

11. Hansen, T. O.; Rehfeld, J. F.; Nielsen, F. C. Cyclic AMP-Induced Neuronal Differentiation via Activation of p38 Mitogen-Activated Protein Kinase. *J. Neurochem*. **2000**, *75*, 1870–1877.

12. Esfandiari, F.; Fathi, A.; Gourabi, H.; et al. Glycogen Synthase Kinase-3 Inhibition Promotes Proliferation and Neuronal Differentiation of Human-Induced Pluripotent Stem Cell-Derived Neural Progenitors. *Stem Cells Dev*. **2012**, *21*, 3233–3243.

13. Lange, C.; Mix, E.; Frahm, J.; et al. Small Molecule GSK-3 Inhibitors Increase Neurogenesis of Human Neural Progenitor Cells. *Neurosci. Lett*. **2011**, *488*, 36–40.

14. Han, J.; Wang, B.; Xiao, Z.; et al. Mammalian Target of Rapamycin (mTOR) Is Involved in the Neuronal Differentiation of Neural Progenitors Induced by Insulin. *Mol. Cell Neurosci*. **2008**, *39*, 118–124.

15. Gross, R. E.; Mehler, M. F.; Mabie, P. C.; et al. Bone Morphogenetic Proteins Promote Astroglial Lineage Commitment by Mammalian Subventricular Zone Progenitor Cells. *Neuron* **1996**, *17*, 595–606.

16. Kim, M. Y.; Kaduwal, S.; Yang, D. H.; et al. Bone Morphogenetic Protein 4 Stimulates Attachment of Neurospheres and Astrogenesis of Neural Stem Cells in Neurospheres via Phosphatidylinositol 3 Kinase-Mediated Upregulation of N-Cadherin. *Neuroscience* **2010**, *170*, 8–15.

17. Nakashima, K.; Takizawa, T.; Ochiai, W.; et al. BMP2-Mediated Alteration in the Developmental Pathway of Fetal Mouse Brain Cells from Neurogenesis to Astrocytogenesis. *Proc. Natl. Acad. Sci. U.S.A*. **2001**, *98*, 5868–5873.

18. Yuan, H.; Chen, R.; Wu, L.; et al. The Regulatory Mechanism of Neurogenesis by IGF-1 in Adult Mice. *Mol. Neurobiol*. **2015**, *51*, 512–522.

19. Chadwick, W.; Mitchell, N.; Caroll, J.; et al. Amitriptyline-Mediated Cognitive Enhancement in Aged 3×Tg Alzheimer's Disease Mice Is Associated with Neurogenesis and Neurotrophic Activity. *PLoS One* **2011**, *6*, e21660.

20. Jang, S.-W.; Liu, X.; Chan, C.-B.; et al. Amitriptyline Is a TrkA and TrkB Receptor Agonist That Promotes TrkA/TrkB Heterodimerization and Has Potent Neurotrophic Activity. *Chem. Biol*. **2009**, *16*, 644–656.

21. Sato, A.; Sunayama, J.; Matsuda, K.; et al. Regulation of Neural Stem/Progenitor Cell Maintenance by PI3K and mTOR. *Neurosci. Lett*. **2010**, *470*, 115–120.

22. Magri, L.; Cambiaghi, M.; Cominelli, M.; et al. Sustained Activation of mTOR Pathway in Embryonic Neural Stem Cells Leads to Development of Tuberous Sclerosis Complex-Associated Lesions. *Cell Stem Cell* **2011**, *9*, 447–462.

23. Magri, L.; Galli, R. mTOR Signaling in Neural Stem Cells: From Basic Biology to Disease. *Cell Mol. Life Sci*. **2013**, *70*, 2887–2898.

24. Pertz, H.; Eich, E. Ergot Alkaloids and Their Derivatives as Ligands for Serotoninergic, Dopaminergic and Adrenergic Receptors. In *Ergot: The Genus Claviceps*; Křen, V., Cvak, L., Eds.; CRC Press. Boca Raton, FL, **1999**, pp. 411–440.

25. Tadori, Y.; Forbes, R. A.; McQuade, R. D.; et al. Functional Potencies of Dopamine Agonists and Antagonists at Human Dopamine D_2 and D_3 Receptors. *Eur. J. Pharmacol*. **2011**, *666*, 43–52.

26. Gobello, C. Dopamine Agonists, Anti-Progestins, Anti-Androgens, Long-Term-Release GnRH Agonists and Anti-Estrogens in Canine Reproduction: A Review. *Theriogenology* **2006**, *66*, 1560–1567.

27. Athanasoulia, A. P.; Sievers, C.; Uhr, M.; et al. The Effect of the *ANKK1/DRD2 Taq1A* Polymorphism on Weight Changes of Dopaminergic Treatment in Prolactinomas. *Pituitary* **2014**, *17*, 240–245.

28. Heilker, R.; Traub, S.; Reinhardt, P.; et al. iPS Cell Derived Neuronal Cells for Drug Discovery. *Trends Pharmacol. Sci*. **2014**, *35*, 510–519.